Enzyme Models

DOI: 10.1002/anie.201000819

Water as an Oxygen Source: Synthesis, Characterization, and Reactivity Studies of a Mononuclear Nonheme Manganese(IV) Oxo Complex**

*Sarvesh C. Sawant, Xiujuan Wu, Jaeheung Cho, Kyung-Bin Cho, Sun Hee Kim, Mi Sook Seo, Yong-Min Lee, Minoru Kubo, Takashi Ogura, Sason Shaik, and Wonwoo Nam**

High-valent manganese oxo species have been invoked as key intermediates in the oxidation of organic substrates by heme and nonheme manganese catalysts, and in water oxidation by the oxygen-evolving complex (OEC) in photosystem II (PS II).[1,2] To elucidate the chemical and physical properties of high-valent manganese oxo intermediates, a number of heme and nonheme Mn^{IV} and Mn^{V} oxo complexes have been synthesized, and characterized by using various spectroscopic methods and X-ray crystallography. The reactivities of these species have also been investigated in oxidation reactions, such as C–H bond activation, olefin epoxidation, halogenation, and hydride- and electron-transfer reactions.[3–9]

In PS II, the oxidation of water by the OEC induces the generation of high-valent Mn^{IV} oxo species by a proton-coupled electron transfer (PCET) mechanism. The oxygen atom in the Mn^{V} oxo intermediate is derived from water.[1] Biomimetic studies have established the formation of ruthenium oxo complexes in water oxidation in the presence of a strong oxidant, such as Ce^{IV} or $[Ru(bpy)_3]^{3+}$ (bpy = 2,2'-bipyridine).[10–12] Very recently, we have generated mononuclear nonheme Fe^{IV} oxo complexes using water as an oxygen source and Ce^{IV} as an one-electron oxidant.[13] Since it has been proposed that high-valent manganese oxo species are generated by the oxidation of water at the OEC of PS II, we attempted to generate high-valent manganese oxo species in a similar fashion.[14] Herein, we report the generation of a mononuclear nonheme Mn^{IV} oxo complex using water as an oxygen source and Ce^{IV} as an one-electron oxidant. The spectroscopic characterization and DFT-optimized structure of the intermediate are also reported. We also report the reactivity of the nonheme Mn^{IV} oxo complex in oxygenation reactions.

Addition of cerium(IV) ammonium nitrate (CAN; 8 mM) to a reaction solution containing $[Mn^{II}(BQCN)](CF_3SO_3)_2$ (**1**; 2 mM; BQCN = *N*,*N*′-dimethyl-*N*,*N*′-bis(8-quinolyl)cyclohexanediamine; see the crystal structure of **1** in Figure 1 and Figures S1, S2 and Tables S1, S2 in the Supporting Information for the synthesis, characterization, and structural data of **1**) gave a green complex **2** with an absorption band at 630 nm ($\varepsilon \approx 400\ M^{-1}\,cm^{-1}$) in CH_3CN/H_2O (9:1) or acetone/H_2O (9:1) at 0 °C ($t_{1/2} \approx 10$ h; Figure 2a). The intermediate **2** was also synthesized by the reaction of **1** with iodosylbenzene (PhIO) in CH_3CN or acetone at −40 °C ($t_{1/2} \approx 1$ h).

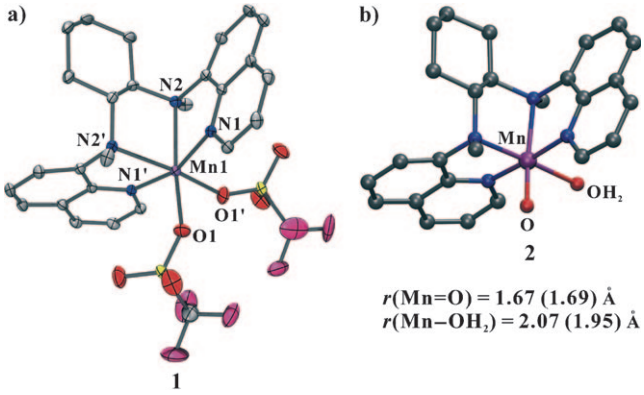

Figure 1. a) X-ray structure of $[Mn^{II}(BQCN)](CF_3SO_3)_2$ (**1**) showing thermal ellipsoids at 30% probability. Hydrogen atoms are omitted for clarity. Selected bond distances [Å]: Mn1–N1 2.2048(16), Mn1–N2 2.3364(16), Mn1–O1 2.1491(16). b) Gas-phase DFT-optimized structure of **2** calculated at the B3LYP/LACVP level. Mulliken spin density distribution: ρ(Mn) = 2.54 (2.65) and ρ(O) = 0.61 (0.50). Values in parentheses indicate results from structures optimized with water cluster $(H_2O)_{16}$ explicitly present.

The intermediate **2** was then characterized by using various spectroscopic methods. EPR spectroscopy was used to demonstrate that **2** has an $S = 3/2$ Mn^{IV} center. The X-band continuous wave (CW) EPR spectrum of **2** shows a broad absorption band at $g_{eff} \approx 4$, which originates from the zero-field splitting of the high-spin d^3 ($S = 3/2$) manganese

[*] Dr. S. C. Sawant, X. Wu, Dr. J. Cho, Dr. K.-B. Cho, Dr. S. H. Kim, Dr. M. S. Seo, Dr. Y.-M. Lee, Prof. Dr. W. Nam
Department of Bioinspired Science
Department of Chemistry and Nano Science and
Centre for Biomimetic Systems
Ewha Womans University, Seoul 120–750 (Korea)
Fax: (+82) 2-3277-4441
E-mail: wwnam@ewha.ac.kr
Dr. M. Kubo, Prof. Dr. T. Ogura
Picobiology Institute, Graduate School of Life Science
University of Hyogo (Japan)
Prof. Dr. S. Shaik
Department of Organic Chemistry and The Lise Meitner-Minerva Center for Computational Quantum Chemistry
The Hebrew University of Jerusalem (Israel)

[**] The research at EWU was supported by NRF/MEST of Korea through the CRI, WCU (R31-2008-000-10010-0), and GRL (2010-00353) Programs (to W.N.). The research at UH was supported by Grant-in-Aid for scientific research (C) (no. 21570171; to T.O.) by MEXT (Japan). S.S. thanks the Israel Science Foundation (Grant 16/06).

Supporting information for this article is available on the WWW under http://dx.doi.org/10.1002/anie.201000819.

compound (Figure 2b).[7b,15] It has been shown that low-field signals are prominent when the axial zero-field splitting (D) is greater than the energy of the incident microwave photon ($h\nu = 0.32\ cm^{-1}$ for 9.68 GHz),[7b,8c,15] which is consistent with our result. The simulated EPR spectrum was consistent with the experimental spectrum when the axial zero-field splitting parameter $D = 2\ cm^{-1}$ and the rhombic zero-field parameter $E/D = 0$ were used (Figure 2b).[16]

The electrospray ionization mass spectrum (ESI MS) of **2** shows prominent ion peaks at m/z 242.5, 263.0, and 484.1, the mass and isotope distribution patterns of which correspond to $[Mn^{IV}(BQCN)(O)(H_2O)]^{2+}$ or $[Mn^{IV}(BQCN)(OH)_2]^{2+}$ (calculated m/z 242.6), $[Mn^{IV}(BQCN)(O)(H_2O)(CH_3CN)]^{2+}$ or $[Mn^{IV}(BQCN)(OH)_2(CH_3CN)]^{2+}$ (calculated m/z 263.1), and $[Mn^{IV}(BQCN)(O)(OH)]^{+}$ (calculated m/z 484.2), respectively. When the reaction was carried out in the presence of isotopically labeled $H_2{}^{18}O$, peaks corresponding to $[Mn^{IV}(BQCN)(^{18}O)(H_2{}^{18}O)]^{2+}$ or $[Mn^{IV}(BQCN)(^{18}OH)_2]^{2+}$, $[Mn^{IV}(BQCN)(^{18}O)(H_2{}^{18}O)(CH_3CN)]^{2+}$ or $[Mn^{IV}(BQCN)(^{18}OH)_2(CH_3CN)]^{2+}$, and $[Mn^{IV}(BQCN)(^{18}O)(^{18}OH)]^{+}$ appeared at m/z 244.5, 265.0, and 488.1, respectively (Figure 2c). The experiment with labeled water thus demonstrates that the oxygen atom in **2** originates from water.

The resonance Raman spectrum of **2**, measured in acetone/H_2O (9:1) at −40 °C with 407 nm laser excitation, showed an isotope-sensitive band at 707 cm^{-1}, which shifted to 676 cm^{-1} when [^{18}O]-**2** was generated in acetone/$H_2{}^{18}O$ (9:1; Figure 2d). The observed isotopic shift of −31 cm^{-1} with ^{18}O substitution is in agreement with the calculated value ($\Delta\nu_{calc} = -31\ cm^{-1}$) for the Mn–O diatomic harmonic oscillator. The observed Mn–O frequency at 707 cm^{-1} is lower than those reported in a nonheme Mn^{IV} oxo complex $[Mn^{IV}(H_3buea)(O)]^{-}$ ($\nu_{Mn=O} = 737\ cm^{-1}$; H_3buea = tris[(*N*′-*tert*-butylureaylato)-*N*-ethylene]aminato),[7b] and Mn^{IV} oxo porphyrin complexes ($\nu_{Mn=O} \approx 750\ cm^{-1}$),[17] but is higher than that observed in a nonheme Mn^{IV} hydroxo complex $[Mn^{IV}(Me_2EBC)(OH)_2]^{2+}$ ($\nu_{Mn-OH} = 664\ cm^{-1}$; Me_2EBC = 4,11-dimethyl-1,4,8,11-tetraazabicyclo[6.6.2]hexadecane).[8a] In the latter case, the Mn–OH band was shifted from 664 cm^{-1} to 660 cm^{-1} when the intermediate was generated in the presence of D_2O.[8a] However, in the present study, we did not observe the isotopic shift when **2** was prepared in the presence of D_2O, thus suggesting that **2** contains a terminal oxo ligand and not hydroxo ligands. Based on the above spectroscopic data, it follows that the intermediate **2** is a Mn^{IV} complex with a terminal oxo ligand that has a double-bond character between the manganese ion and oxygen atoms, and that the oxygen atom in the Mn^{IV} oxo species originates from water [Eq. (1)].

$$[(BQCN)Mn^{II}-OH_2]^{2+} \xrightarrow{-2e^-,\ -2H^+} [(BQCN)Mn^{IV}=O]^{2+} \quad (1)$$

DFT calculations at B3LYP/LACV3P*$^{+}$//B3LYP/LACVP level[18] were performed to elucidate the structural details of **2** (Figure 1b) and to compare the relative energy of **2** to its structural tautomer $[Mn^{IV}(BQCN)(OH)_2]^{2+}$ (**3**; see the Supporting Information for technical details). The calculations show that the solvating water molecules play a key role in the formation of **2** from the tautomer **3**. For instance, when

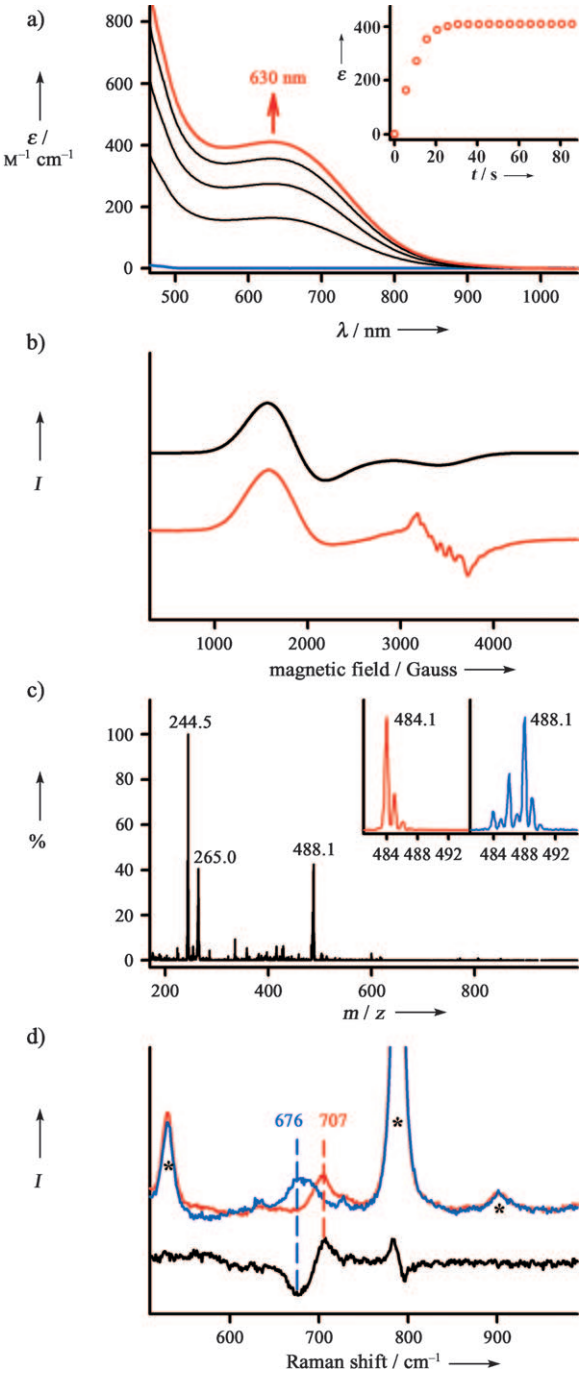

Figure 2. a) UV/Vis spectral changes showing the formation of **2** (red line) in the reaction of **1** (2 mM; blue line) and $[Ce^{IV}(NO_3)_6](NH_4)_2$ (8 mM) in CH_3CN/H_2O (9:1) at 0 °C. The inset shows the time course of the formation of **2** monitored at 630 nm. b) X-band CW-EPR spectrum (red line) of **2** recorded at 5 K and the simulated spectrum (black line). The hyperfine splitting (ca. 95 G) observed at $g \approx 2$ results from a minor impurity of Mn^{II} species. c) ESI MS of [^{18}O]-**2** formed in the reaction of **1** and CAN (4 equiv) in $CH_3CN/H_2{}^{18}O$ (9:1) at 0 °C. The insets show the observed isotope distribution patterns for [^{16}O]-**2** (left panel, prepared with $H_2{}^{16}O$) and [^{18}O]-**2** (right panel, prepared with $H_2{}^{18}O$). d) Resonance Raman spectra (407 nm excitation) of [^{16}O]-**2** (red line) generated in the reaction of **1** (4 mM) and 4 equiv of CAN in acetone/$H_2{}^{16}O$ mixture (9:1) and [^{18}O]-**2** (blue line) formed in acetone/$H_2{}^{18}O$ mixture (9:1) at −40 °C. The black line shows the intensity difference between the two spectra. * indicates peaks that arise from the solvent.

comparing the gas-phase energies of **2** and **3**, the calculations clearly predicted **3** to be lower in energy (in the order of 12 kcal mol^{-1}, see the Supporting Information). However, upon addition of a water cluster with randomly distributed water molecules around the oxygen ligands, **3** no longer exists as an energy minimum. Instead, **3** spontaneously loses a proton to the solution to form $[Mn^{IV}(BQCN)(O)(HO)]^+$ and H_3O^+. This Mn^{IV} species is computed to be about 1 kcal mol^{-1} higher in free energy than **2** (Table S6 in the Supporting Information). Furthermore, since the reaction mixture becomes acidic in the presence of cerium ions, protonation of the Mn–OH group to form **2** is entirely plausible and the corresponding optimized structure is the one as shown in Figure 1b (see also Figure S7b in the Supporting Information). The calculated Mn=O bond length in **2** is 1.67/1.69 Å (gas phase/solvated). This bond length is similar to that found in $[Mn^{IV}(H_3buea)(O)]^-$ (1.706 Å; determined by DFT calculations)[7b] and those found in Mn^{IV} or Mn^{V} oxo porphyrins (ca. 1.68 Å; determined by EXAFS analysis),[4b,19] in which the Mn–O bond has a double-bond character.

The oxidative reactivity of **2** was explored in the C–H bond activation of alkyl-subsituted aromatic compounds and in the oxidation of aromatic compounds and benzyl alcohol. Upon reaction with substrates such as xanthene, 9,10-dihydroanthracene (DHA), 1,4-cyclohexadiene (CHD), and fluorene, which have bond dissociation energies (BDEs) in the range of 75.5–80 kcal mol^{-1},[20] **2** was consumed with a pseudo-first-order decay (Figure 3a; see also the Experimental Section in the Supporting Information for product analysis). The pseudo-first-order rate constants increased proportionally with substrate concentration (Figure S3 in the Supporting Information), from which second-order rate constants k_2 were determined. The corresponding $\log k_2'$ values gave a linear correlation with the BDEs of the substrates (Figure 3b). Furthermore, a kinetic isotope effect (KIE) value of 3.4(3) was observed in the oxidation of xanthene by **2**. This value is much smaller than those obtained in the oxidation of xanthene by a Mn^{IV} oxo porphyrin complex (KIE value of 14)[4d] and nonheme Fe^{IV} oxo complexes (KIE values of 10–20),[21] but is similar to those obtained in the oxidation of DHA by $[Mn^{IV}(Me_2EBC)(OH)_2]^{2+}$ (KIE value of 3.3) and $Mn^{IV}(Me_2EBC)(O)_2$ (KIE value of 3.78).[8c] Based on the correlation between reaction rates and BDEs of substrates and the significant KIE value, we conclude that the C–H bond activation by **2** occurs by an H-atom abstraction mechanism.

The Mn^{IV} oxo species **2** was also found to hydroxylate anthracene and *para*-substituted anthracene derivatives. With anthracene, the reaction rates increased proportionally with the substrate concentration to give a second-order rate constant of $2.0(2)\times10^{-1}\,M^{-1}s^{-1}$ at 0 °C (Figure S4 and Experimental Section in the Supporting Information). The electronic effect of the anthracene substituent is apparent from Figure 3c, which shows a good linear correlation with the σ_p of the substituents (i.e., a negative Hammett ρ value of −1.8(2)), thus indicating that the manganese oxo group attacks the aromatic ring by an electrophilic pathway. We noted that negative Hammett ρ values of −3.9 and −8.0 were observed in aromatic hydroxylation reactions by nonheme

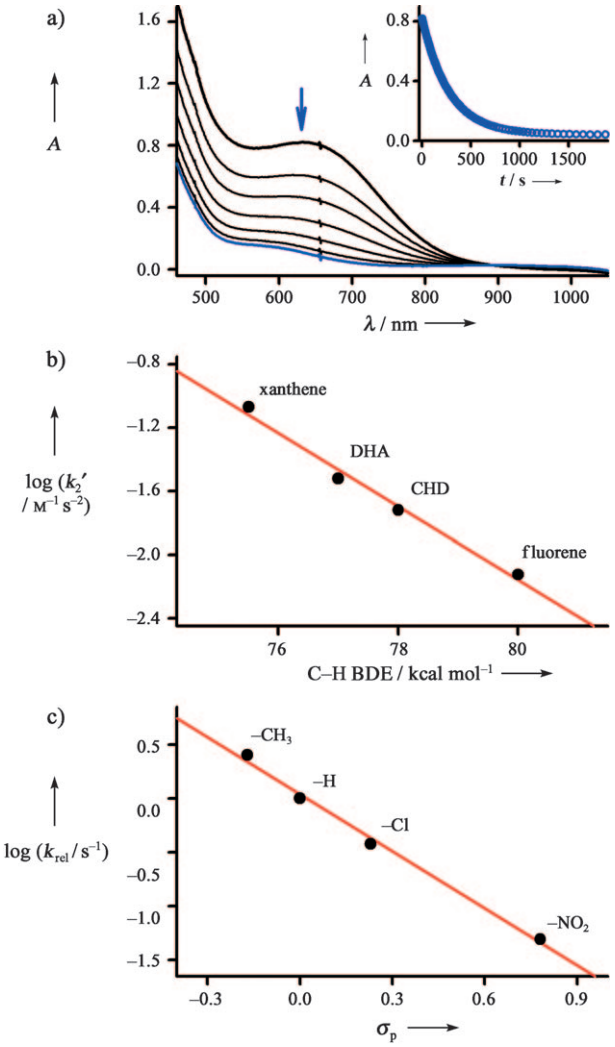

Figure 3. a) Changes in the UV/Vis spectrum of **2** (2 mM) upon addition of xanthene (10 equiv, 20 mM) in CH_3CN/H_2O (9:1) at 0 °C. Inset shows the time course of the decay of **2** monitored at 630 nm. b) Plot of $\log k_2'$ of **2** against the C–H BDE of substrates, such as xanthene (75.5 kcal mol^{-1}), DHA (77 kcal mol^{-1}), CHD (78 kcal mol^{-1}), and fluorene (80 kcal mol^{-1}). Second-order rate constants k_2 were determined at 0 °C and then adjusted for reaction stoichiometry to yield k_2' based on the number of equivalent target C–H bonds of substrates (e.g., 2 for xanthene and fluorene and 4 for DHA and CHD). c) Hammett plot of $\log k_{rel}$ against σ_p of anthracene derivatives in the reactions of **2** (1 mM) with *para*-substituted anthracene derivatives (10 equiv with respect to **2**) at 0 °C.

Fe^{IV} oxo and Fe^{IV} oxo porphyrin π-cation radical complexes, respectively.[22] Furthermore, a KIE value of 0.98(2) was determined in the hydroxylation of undeuterated and deuterated anthracene derivatives by **2** (Figure S4 in the Supporting Information), thus indicating the addition of an electrophilic manganese oxo group to the sp^2 center of aromatic ring to form a σ adduct.[22,23]

Finally, the intermediate **2** was shown to oxidize benzyl alcohol to give benzaldehyde as a major product (ca. 90% yield based on the intermediate generated), with a second-order rate constant of $4.4(3)\times10^{-3}\,M^{-1}s^{-1}$ at 0 °C (Figure S5 in

the Supporting Information). The benzyl alcohol oxidation was also carried out with deuterated benzyl alcohol ($C_6D_5CD_2OH$), for which a KIE value of 2.1 was obtained. This KIE value is similar to that obtained in an intermolecular competitive oxidation of benzyl alcohol and deuterated benzyl alcohol (KIE value of 2.2) by a nonheme manganese(II) catalyst, $[Mn^{II}(BQEN)]^{2+}$ (BQEN=*N*,*N*′-dimethyl-*N*,*N*′-bis(8-quinolyl)ethane-1,2-diamine) and peracetic acid under catalytic conditions,[24] thus suggesting that an Mn^{IV} oxo species might be involved as a reactive intermediate in the manganese(II)-complex-catalyzed oxidation of organic substrates by peracetic acid.[24,25] Moreover, the KIE value of 2.1 is much smaller than those determined in the oxidation of benzyl alcohol by nonheme Fe^{IV} oxo complexes (e.g., a KIE value of ca. 50).[26]

In conclusion, we have demonstrated the generation of a mononuclear nonheme Mn^{IV} oxo complex in a reaction using water as an oxygen source and Ce^{IV} as an oxidant; the source of oxygen in the manganese oxo complex was assigned unambiguously by carrying out experiments with isotopically labeled water. The intermediate was characterized by using various spectroscopic methods, and DFT calculations confirm that this species is indeed energetically accessible and not sufficiently basic to undergo protonation on the Mn=O unit. Our findings also show that the Mn^{IV} oxo complex is an effective oxidant in oxidation reactions.

Received: February 10, 2010
Revised: August 27, 2010
Published online: September 21, 2010

Keywords: bioinorganic chemistry · enzyme models · manganese · oxygenation · reaction mechanisms

[1] a) J. P. McEvoy, G. W. Brudvig, *Chem. Rev.* **2006**, *106*, 4455 – 4483; b) T. J. Meyer, M. H. V. Huynh, H. H. Thorp, *Angew. Chem.* **2007**, *119*, 5378 – 5399; *Angew. Chem. Int. Ed.* **2007**, *46*, 5284 – 5304; c) V. L. Pecoraro, W.-Y. Hsieh, *Inorg. Chem.* **2008**, *47*, 1765 – 1778; d) J. Barber, *Chem. Soc. Rev.* **2009**, *38*, 185 – 196; e) W. Lubitz, E. J. Reijerse, J. Messinger, *Energy Environ. Sci.* **2008**, *1*, 15 – 31.

[2] a) B. Meunier, A. Robert, G. Pratviel, J. Bernadou in *The Porphyrin Handbook*, *Vol. 4* (Eds.: K. M. Kadish, K. M. Smith, R. Guilard), Academic Press, San Diego, **2000**, pp. 119 – 187; b) J. T. Groves in *Cytochrome P450: Structure, Mechanism, and Biochemistry*, 3rd ed. (Ed.: P. R. Ortiz de Montellano), Kluwer Academic/Plenum Publishers, New York, **2005**, pp. 1 – 43.

[3] a) J. T. Groves, J. Lee, S. S. Marla, *J. Am. Chem. Soc.* **1997**, *119*, 6269 – 6273; b) N. Jin, J. T. Groves, *J. Am. Chem. Soc.* **1999**, *121*, 2923 – 2924; c) N. Jin, J. L. Bourassa, S. C. Tizio, J. T. Groves, *Angew. Chem.* **2000**, *112*, 4007 – 4009; *Angew. Chem. Int. Ed.* **2000**, *39*, 3849 – 3851; d) F. De Angelis, N. Jin, R. Car, J. T. Groves, *Inorg. Chem.* **2006**, *45*, 4268 – 4276; e) N. Jin, M. Ibrahim, T. G. Spiro, J. T. Groves, *J. Am. Chem. Soc.* **2007**, *129*, 12416 – 12417.

[4] a) W. Nam, I. Kim, M. H. Lim, H. J. Choi, J. S. Lee, H. G. Jang, *Chem. Eur. J.* **2002**, *8*, 2067 – 2071; b) W. J. Song, M. S. Seo, S. D. George, T. Ohta, R. Song, M.-J. Kang, T. Tosha, T. Kitagawa, E. I. Solomon, W. Nam, *J. Am. Chem. Soc.* **2007**, *129*, 1268 – 1277; c) J. Y. Lee, Y.-M. Lee, H. Kotani, W. Nam, S. Fukuzumi, *Chem. Commun.* **2009**, 704 – 706; d) C. Arunkumar, Y.-M. Lee, J. Y. Lee, S. Fukuzumi, W. Nam, *Chem. Eur. J.* **2009**, *15*, 11482 – 11489; e) S. Fukuzumi, N. Fujioka, H. Kotani, K. Ohkubo, Y.-M. Lee, W. Nam, *J. Am. Chem. Soc.* **2009**, *131*, 17127 – 17134.

[5] a) R. Zhang, M. Newcomb, *J. Am. Chem. Soc.* **2003**, *125*, 12418 – 12419; b) R. Zhang, J. H. Horner, M. Newcomb, *J. Am. Chem. Soc.* **2005**, *127*, 6573 – 6582.

[6] Y. Shimazaki, T. Nagano, H. Takesue, B.-H. Ye, F. Tani, Y. Naruta, *Angew. Chem.* **2004**, *116*, 100 – 102; *Angew. Chem. Int. Ed.* **2004**, *43*, 98 – 100.

[7] a) R. L. Shook, A. S. Borovik, *Inorg. Chem.* **2010**, *49*, 3646 – 3660; b) T. H. Parsell, M.-Y. Yang, A. S. Borovik, *J. Am. Chem. Soc.* **2009**, *131*, 2762 – 2763; c) T. H. Parsell, R. K. Behan, M. T. Green, M. P. Hendrich, A. S. Borovik, *J. Am. Chem. Soc.* **2006**, *128*, 8728 – 8729.

[8] a) G. Yin, J. M. McCormick, M. Buchalova, A. M. Danby, K. Rodgers, V. W. Day, K. Smith, C. M. Perkins, D. Kitko, J. D. Carter, W. M. Scheper, D. H. Busch, *Inorg. Chem.* **2006**, *45*, 8052 – 8061; b) G. Yin, A. M. Danby, D. Kitko, J. D. Carter, W. M. Scheper, D. H. Busch, *J. Am. Chem. Soc.* **2007**, *129*, 1512 – 1513; c) G. Yin, A. M. Danby, D. Kitko, J. D. Carter, W. M. Scheper, D. H. Busch, *J. Am. Chem. Soc.* **2008**, *130*, 16245 – 16253; d) T. Kurahashi, A. Kikuchi, T. Tosha, Y. Shiro, T. Kitagawa, H. Fujii, *Inorg. Chem.* **2008**, *47*, 1674 – 1686; e) T. Kurahashi, A. Kikuchi, Y. Shiro, M. Hada, H. Fujii, *Inorg. Chem.* **2010**, *49*, 6664 – 6672.

[9] a) T. J. Collins, R. D. Powell, C. Slebodnick, E. S. Uffelman, *J. Am. Chem. Soc.* **1990**, *112*, 899 – 901; b) F. M. MacDonnell, N. L. P. Fackler, C. Stern, T. V. O'Halloran, *J. Am. Chem. Soc.* **1994**, *116*, 7431 – 7432.

[10] a) X. Sala, I. Romero, M. Rodríguez, L. Escriche, A. Llobet, *Angew. Chem.* **2009**, *121*, 2882 – 2893; *Angew. Chem. Int. Ed.* **2009**, *48*, 2842 – 2852; b) S. Romain, L. Vigara, A. Llobet, *Acc. Chem. Res.* **2009**, *42*, 1944 – 1953; c) F. Liu, J. J. Concepcion, J. W. Jurss, T. Cardolaccia, J. L. Templeton, T. J. Meyer, *Inorg. Chem.* **2008**, *47*, 1727 – 1752; d) J. K. Hurst, J. L. Cape, A. E. Clark, S. Das, C. Qin, *Inorg. Chem.* **2008**, *47*, 1753 – 1764.

[11] a) Y. Hirai, T. Kojima, Y. Mizutani, Y. Shiota, K. Yoshizawa, S. Fukuzumi, *Angew. Chem.* **2008**, *120*, 5856 – 5860; *Angew. Chem. Int. Ed.* **2008**, *47*, 5772 – 5776; b) C.-M. Che, V. W.-W. Yam, T. C. W. Mak, *J. Am. Chem. Soc.* **1990**, *112*, 2284 – 2291.

[12] a) F. Bozoglian, S. Romain, M. Z. Ertem, T. K. Todorova, C. Sens, J. Mola, M. Rodríguez, I. Romero, J. Benet-Buchholz, X. Fontrodona, C. J. Cramer, L. Gagliardi, A. Llobet, *J. Am. Chem. Soc.* **2009**, *131*, 15176 – 15187; b) A. Sartorel, M. Carraro, G. Scorrano, R. De Zorzi, S. Geremia, N. D. McDaniel, S. Bernhard, M. Bonchio, *J. Am. Chem. Soc.* **2008**, *130*, 5006 – 5007; c) Y. V. Geletii, B. Botar, P. Kögerler, D. A. Hillesheim, D. G. Musaev, C. L. Hill, *Angew. Chem.* **2008**, *120*, 3960 – 3963; *Angew. Chem. Int. Ed.* **2008**, *47*, 3896 – 3899; d) J. A. Gilbert, D. S. Eggleston, W. R. Murphy, Jr., D. A. Geselowitz, S. W. Gersten, D. J. Hodgson, T. J. Meyer, *J. Am. Chem. Soc.* **1985**, *107*, 3855 – 3864.

[13] Y.-M. Lee, S. N. Dhuri, S. C. Sawant, J. Cho, M. Kubo, T. Ogura, S. Fukuzumi, W. Nam, *Angew. Chem.* **2009**, *121*, 1835 – 1838; *Angew. Chem. Int. Ed.* **2009**, *48*, 1803 – 1806.

[14] For the synthesis of a mononuclear nonheme Mn^{III} oxo complex using water as an oxygen source, see: a) R. Gupta, C. E. MacBeth, V. G. Young, Jr., A. S. Borovik, *J. Am. Chem. Soc.* **2002**, *124*, 1136 – 1137; b) C. E. MacBeth, R. Gupta, K. R. Mitchell-Koch, V. G. Young, Jr., G. H. Lushington, W. H. Thompson, M. P. Hendrich, A. S. Borovik, *J. Am. Chem. Soc.* **2004**, *126*, 2556 – 2567; c) A. S. Borovik, *Acc. Chem. Res.* **2005**, *38*, 54 – 61.

[15] a) K. A. Campbell, M. R. Lashley, J. K. Wyatt, M. H. Nantz, R. D. Britt, *J. Am. Chem. Soc.* **2001**, *123*, 5710 – 5719; b) D. P. Kessissoglou, X. Li, W. M. Butler, V. L. Pecoraro, *Inorg. Chem.* **1987**, *26*, 2487 – 2492.

[16] Spectral simulations were carried out using EasySpin 3.0: S. Stoll, A. Schweiger, *J. Magn. Reson.* **2006**, *178*, 42 – 55.
[17] a) R. S. Czernuszewicz, Y. O. Su, M. K. Stern, K. A. Macor, D. Kim, J. T. Groves, T. G. Spiro, *J. Am. Chem. Soc.* **1988**, *110*, 4158 – 4165; b) R. Makino, T. Uno; Y. Nishimura, T. Iizuka, M. Tsuboi, Y. Ishimura, *J. Biol. Chem.* **1986**, *261*, 8376 – 8382.
[18] a) A. D. Becke, *Phys. Rev. A* **1988**, *38*, 3098 – 3100; b) A. D. Becke, *J. Chem. Phys.* **1993**, *98*, 1372 – 1377; c) A. D. Becke, *J. Chem. Phys.* **1993**, *98*, 5648 – 5652; d) C. Lee, W. Yang, R. G. Parr, *Phys. Rev. B* **1988**, *37*, 785 – 789; e) P. J. Hay, W. R. Wadt, *J. Chem. Phys.* **1985**, *82*, 299 – 310.
[19] K. Ayougou, E. Bill, J. M. Charnock, C. D. Garner, D. Mandon, A. X. Trautwein, R. Weiss, H. Winkler, *Angew. Chem.* **1995**, *107*, 370 – 373; *Angew. Chem. Int. Ed. Engl.* **1995**, *34*, 343 – 346.
[20] a) W. W. Y. Lam, W.-L. Man, T.-C. Lau, *Coord. Chem. Rev.* **2007**, *251*, 2238 – 2252; b) J. M. Mayer, *Biomimetic Oxidations Catalyzed by Transition Metal Complexes* (Ed.: B. Meunier), Imperial College Press, London, **2000**, pp. 1 – 43; c) J. P. Roth, J. M. Mayer, *Inorg. Chem.* **1999**, *38*, 2760 – 2761.
[21] C. V. Sastri, J. Lee, K. Oh, Y. J. Lee, J. Lee, T. A. Jackson, K. Ray, H. Hirao, W. Shin, J. A. Halfen, J. Kim, L. Que, Jr., S. Shaik, W. Nam, *Proc. Natl. Acad. Sci. USA* **2007**, *104*, 19181 – 19186.
[22] a) S. P. de Visser, K. Oh, A.-R Han, W. Nam, *Inorg. Chem.* **2007**, *46*, 4632 – 4641; b) M.-J. Kang, W. J. Song, A.-R. Han, Y. S. Choi, H. G. Jang, W. Nam, *J. Org. Chem.* **2007**, *72*, 6301 – 6304.
[23] S. P. de Visser, S. Shaik, *J. Am. Chem. Soc.* **2003**, *125*, 7413 – 7424.
[24] K. Nehru, S. J. Kim, I. Y. Kim, M. S. Seo, Y. Kim, S.-J. Kim, J. Kim, W. Nam, *Chem. Commun.* **2007**, 4623 – 4625.
[25] a) A. Murphy, G. Dubois, T. D. P. Stack, *J. Am. Chem. Soc.* **2003**, *125*, 5250 – 5251; b) A. Murphy, A. Pace, T. D. P. Stack, *Org. Lett.* **2004**, *6*, 3119 – 3122.
[26] N. Y. Oh, Y. Suh, M. J. Park, M. S. Seo, J. Kim, W. Nam, *Angew. Chem.* **2005**, *117*, 4307 – 4311; *Angew. Chem. Int. Ed.* **2005**, *44*, 4235 – 4239.

